

The eJWST active galactic nucleus observation catalogue

V. Lenk^{1,2}, A. Labiano³, C. Circosta^{4,5}, A. Alonso-Herrero⁵, and D. Wylezalek¹

¹ Zentrum für Astronomie der Universität Heidelberg, Astronomisches Rechen-Institut Mönchhofstr, 12-14 69120 Heidelberg, Germany. e-mail: virginialenk@gmx.de

² European Space Agency (ESA), European Space Astronomy Centre (ESAC), Camino Bajo del Castillo s/n, 28692 Villanueva de la Cañada, Madrid, Spain.

³ Telespazio UK S.L. for ESA, ESAC, Camino Bajo del Castillo s/n, 28692 Villanueva de la Cañada, Madrid, Spain.

⁴ Institut de Radioastronomie Millimétrique (IRAM), 300 rue de la Piscine, 38400 Saint-Martin-d'Hères, France.

⁵ Centro de Astrobiología (CAB), CSIC-INTA, Camino Bajo del Castillo s/n, 28692 Villanueva de la Cañada, Spain.

Received ..., 2025; accepted ..., 2025

ABSTRACT

Context. The European Archive of the *James Webb* Space Telescope (eJWST) provides access to all data collected by the *James Webb* Space Telescope (JWST). JWST's capabilities span from studying early Universe galaxy formation to probing exoplanet atmospheres. Specifically, for active galactic nuclei (AGNs), JWST offers unparalleled opportunities, enabling investigation into AGN phenomena with unprecedented detail through high-resolution imaging, spectroscopy, and photometric data.

Aims. This study aims to compile and release a catalogue of all AGN observations conducted with JWST. Using eJWST, we systematically filtered and organized these observations to facilitate access and retrieval of all of JWST's data products related to AGNs. Our goal is to provide the community with a valuable resource for their research.

Methods. We compiled the AGN observations in eJWST using specific keywords set by the principal investigators in their proposals, manually reviewing the approved programmes of JWST, as well as cross-matching all available observations with available AGN catalogues, such as the Million Quasar catalogue, the SDSS MaNGA AGN catalogue, the CDFS catalogue, and others.

Results. The resulting catalogue contains a total of 3,242 individual AGNs included in JWST observations. This is one of the first extensive collections of AGN observations from the JWST. It includes detailed information about the targets (name, coordinates, and redshift) and specifics of the JWST observations (instrument, aperture, filter, etc.), and provides links for data downloads.

Conclusions.

Key words. Catalogs, Galaxies: active

1. Introduction

The *James Webb* Space Telescope (JWST), launched in December 2021, is a space infrared observatory built by the National Aeronautics and Space Administration (NASA), the European Space Agency (ESA), and the Canadian Space Agency (CSA). It represents a monumental advancement in astronomical observation, providing extraordinary sensitivity and wavelength coverage from 0.6 to 28 microns (Gardner et al. 2023; Rigby et al. 2023). JWST is equipped with four scientific instruments: the Near Infrared Camera (NIRCam; Rieke et al. 2005; Rieke et al. 2023), the Near Infrared Spectrograph (NIRSpec; Ferruit 2012; Böker et al. 2023), the Mid-Infrared Instrument (MIRI; Rieke 2015; Wright et al. 2015, 2023), and the Fine Guidance Sensor/Near InfraRed Imager and Slitless Spectrograph (FGS/NIRISS; Doyon 2012; Doyon et al. 2023). The telescope transmits $\gtrsim 28.6$ Gb of data to Earth twice per day¹. These data are then sent to the Deep Space Network (DSN), a global network of large radio antennas located in Goldstone, California, Madrid, Spain, and Canberra, Australia. After the accumulation of data on the ground, they are transmitted to the Space Telescope Science Institute (STScI) in Baltimore (Swade et al. 2014; Greene et al. 2015). There, the Data Management System (DMS) processes them to three different calibration lev-

els: Calibration Level 1 is the initial stage of the JWST data pipeline. At this level, basic calibration corrections for instrumental effects, such as dark current or the flagging of known bad pixels, are applied. The output consists of count-rate images for each exposure. Calibration Level 2 is the second stage of the pipeline, where further processing of Level 1 data occurs. This includes pixel flat-fielding, derivation, and attachment of world-coordinate information. The output at this stage includes fully calibrated data from individual exposures. The final stage of the pipeline is Calibration Level 3, where individual exposures of Calibration Level 2 are joined to science-ready mosaics, integral field unit (IFU) data cubes, or one-dimensional spectra (Bushouse 2020). Planned observations that have been approved but not yet executed are not part of the calibration pipeline, but they are listed in the archives under Calibration Level -1.

The DMS uses software pipelines designed to handle each of the various modes of operation of the science instruments on board the telescope. These pipelines are frequently updated as the instrument's behaviour, calibration, and knowledge evolve. At the time of writing, the latest available JWST pipeline is 1.17.0 (Bushouse et al. 2024).

After processing, the data are archived in long-term storage systems (archives) and made available to researchers. The three agencies involved in the development of the mission host JWST data archives with different functionalities: the European

¹ <https://jwst-docs.stsci.edu/jwst-general-support> and Gardner et al. (2023)

Table 1. AGN descriptions available in APT for Cycle 4 proposals.

Quasars	Active galactic nuclei	Radio jets
Double quasars	Active galaxies	Radio cores
Radio loud quasars	Seyfert galaxies	Radio lobes
Radio quiet quasars	Blazars	Radio galaxies
X-ray quasars	LINER galaxies	Radio plumes
Broad-absorption line quasar	Galactic accretion disk	Radio hot spots
Quasar-galaxy pairs	Ultraluminous infrared galaxies	Galaxy jets
Relativistic jets	BL Lacertae objects	

archive of the *James Webb* Space Telescope (eJWST²; e.g. [Labiano et al. 2023](#); [Arevalo et al. 2024](#)) at the European Space Astronomy Centre (ESAC), the Mikulski Astronomical Space Telescope (MAST) at the STScI, and the JWST archive at the Canadian Astronomical Data Centre (CADC). The three archives use the same common archive observation model (CAOM; [Dowler 2012](#)) to read and access JWST metadata, so identical versions of every file are hosted on the three sites.

The eJWST is designed to be a service to the European scientific community but is open to all scientists around the world, enabling direct and efficient access to all the JWST science data products. The eJWST forms part of ESA's science archives. It is therefore searchable in combination with data from any other ESA science mission. The eJWST holdings consist of all public data from the JWST mission, as well as access to all proprietary data. The eJWST provides multiple methods for searching for and filtering products and calibration data, such as downloading directly from the user interface or using Astronomical Data Query Language (ADQL; [Mantelet et al. 2023](#)), Astroquery ([Ginsburg et al. 2019](#)), CURL, Python, or WGET queries.

One of the primary goals for the JWST is to study galaxy evolution over time. In this context, active galactic nuclei (AGNs) play a crucial role by influencing the evolution of different properties of their host galaxy ([Graham et al. 2011](#); [Wagner et al. 2012](#); [Silk 2013](#); [Kormendy & Ho 2013](#); [Harrison 2017](#); [Cresci & Maiolino 2018](#); [Circosta et al. 2021](#)). The JWST observations have opened a new window for AGN studies, offering significant advances in resolution and sensitivity at infrared wavelengths, and enable the detection of distant and faint AGNs or AGNs that were previously undetected (e.g. too faint or obscured by dust; [Harikane et al. 2023](#); [Lyu et al. 2024](#)). Over the years, the list of AGNs has increased steadily, as shown by the releases of numerous catalogues such as the Two-degree Field Galaxy Redshift Survey (2dF) catalogue ([Croom et al. 2001](#)), the Sloan Digital Sky Survey (SDSS; [Abazajian et al. 2003](#)), and the 7Ms catalogue of the *Chandra* Deep Field-South Survey (CDFS; [Luo et al. 2017](#)), which resulted in large data collections of AGNs. Creating a comprehensive catalogue of AGNs observed by JWST will be helpful for scientists aiming to explore the impact of nuclear activity on galaxy evolution.

Here we present a catalogue of all the JWST observations of AGNs to date. To create the list of AGNs, we filtered observations directly described as AGNs by the proposers and cross-matched AGN catalogues from the literature with all data in eJWST to provide the community with a comprehensive list of targets and observation modes used to observe them. In Sect. 2 we give a brief introduction on how to access data stored in the eJWST and how to extract datasets. In Sect. 3 we describe the search and filtering processes used to create the catalogue. For the redshift cross-match in this section, we assume a flat Λ cold dark matter cosmology with $H_0 = 70 \text{ km s}^{-1}\text{Mpc}^{-1}$, $\Omega_m = 0.3$,

and $\Omega_\Lambda = 0.7$. In Sect. 4 we describe the different caveats identified throughout the process. In Sect. 5 we discuss objects whose statuses are currently under debate and ongoing surveys that have not yet been included. Then we give an overview of the catalogue and its content in Sect. 6, and recap our work in Sect. 7.

2. Data access in eJWST

There are six different types of JWST observational programmes: the General Observer (GO) programme, the Guaranteed Time Observations programme, the Director's Discretionary Time (DDT), the Director's Discretionary Early Release Science (DD-ERS), the Calibration programmes (which include commissioning data), and the Early Release Observations. Each observation from these programmes is accompanied by data products such as high-resolution images, spectra, or time-series observations, all made publicly available at the JWST archives. The eJWST can be accessed either through the web interface or through a TAP+ REST service ([Dowler et al. 2019](#)). Through the TAP+ service users can query metadata and datasets using the ADQL ([Mantelet et al. 2023](#)).

In this work we made use of this service through the `astroquery.esa.jwst` package in Python, which allowed us to perform ADQL queries (example in Listing 1) to access the metadata directly from eJWST. The eJWST provides several different CAOM tables, storing raw data as well as various calibration levels of observation data. Predominantly, the `jwst.observation` table (the main CAOM observation table) and the `jwst.archive` table (housing data visible on the eJWST archive) were used for this catalogue. From the `jwst.observation` table, we extracted mainly keywords storing instrument (`instrument_keywords`) and target (`target_keywords`) information, while the `jwst.archive` table was used to extract information on the observation itself, such as the process level (`calibrationlevel`), availability to the public (`public`), and metadata release date (`metorelease`). This was necessary because some keywords were exclusive to one table. Upon query execution, data were obtained in the form of an `astropy.table` object, subsequently converted into a PandasDataframe using the Python package Pandas ([pandas development team 2024](#)).

3. AGN selection in eJWST

The goal of this work is to compile a catalogue of all observations with JWST where an AGN is present in the field of view (FoV). Therefore, it is necessary to include not only data from proposals specifically targeting AGNs (throughout the paper we refer to them as 'targeted AGNs'), but also any data where an AGN was within the FoV regardless of the primary objective of

² <https://jwst.esac.esa.int/archive>

the observation ('non-targeted AGNs'). This includes not only science observations, but also calibration and background data.

All archive searches incorporated both public and private science-ready products (calibration level 3) as well as proposed observations (calibration level -1). To ensure that all AGN observations, whether targeted or not, were included in the catalogue, three different methods were applied:

- Search by keywords in the proposals.
- Search within approved programmes.
- Cross-match AGN catalogues with the FoVs of individual JWST observations.

The first two methods (Sects. 3.1 and 3.2) compile a list of all targeted AGNs, while the third method (Sect. 3.3) includes both targeted and non-targeted AGNs. The three methods were then cross-checked to find matches within different catalogues and to eliminate duplicated targets (see Sect. 4). The following subsections describe each method in detail.

3.1. By keywords from proposals

The Astronomer’s Proposal Tool (APT)³ has the option of adding a category and description label to the targets in the proposal. These labels are stored in the CAOM tables. They are accessible through the keyword `target_keywords`, which stores target-specific information separated by a vertical bar ‘|’ (see Fig. 1). Here, the target category and description are found in two versions: the labels `TARGCAT` and `TARGDESC` are used for already observed objects, and `TARGETCATEGORY|` and `TARGETKEYWORDS` for proposed objects (calibration level -1). The `TARGCAT` and `TARGETCATEGORY` labels describe the category of the target (e.g. galaxy, star, etc.), each target being assigned a single category. `TARGDESC` and `TARGETKEYWORDS` provide the target description (e.g. AGNs, protostars, etc.), with the potential for multiple descriptions per target.

We selected all AGN descriptors (see Table 1) from the category ‘Galaxy’ in the proposal parameters documentation⁴ to search for all targeted AGNs in the eJWST. It is important to acknowledge that some targets lack a description entirely (see Sect. 3.2) especially in early data (commissioning and Cycle 1 mainly). These targets lack the descriptor not only in the CAOM tables but also in the flexible image transport system files, and were thus missed by this search method. To complete the sample with these targets, we used the method described in Sect. 3.2.

The target description and categories used for filtering may need to be updated in future catalogue releases if new target descriptions or categories are added to the APT in the next Calls for Proposals. We found 901 individual targeted AGNs using this method.

3.2. By approved programmes

The target descriptions retrieved from the aforementioned keywords are dependent on the proposers' input. As a result, we could not assume that targets were consistently labelled as AGNs, especially since sometimes targets lacked the description field. Also, some AGN sources can fall under different descriptors (e.g. starburst or high-redshift galaxy) and are not labelled as AGNs in the APT field. To address possibly missed AGNs, we implemented an additional search. We searched the approved STScI JWST listed programmes⁵ for additional AGNs, described either in the abstract or elsewhere in the proposal. Specifically, we checked the GO and the Guaranteed Time Observation programmes during all available cycles, as well as the ERS programmes, the DDT, and the calibration programmes. From the GO we checked all the proposals listed under 'Galaxies' and 'Supermassive Black Holes and Active Galaxies'. Naturally, some of these proposals include targets already found in our previous search. We cross-checked the two searches and removed duplicated results. This search method increased our sample to 968 targeted AGNs.

3.3. Cross-matching with AGN catalogues

The high sensitivity of JWST, and the large FoV of some of its instruments, make it possible to detect serendipitous AGNs in the FoV of any observation, regardless of the primary objective of the data (science, calibration, background, etc) or scientific goal of the observation. To build the most complete catalogue of sources we need to include those serendipitous, non-targeted AGNs in the catalogue. The coordinates describing the FoV for any JWST observation are stored in the `position_bounds_spoly` column of the `jwst.archive` table. This column contains four coordinate pairs (RA, Dec) that outline a polygon in the sky.

To account for these non-targeted sources, we cross-matched all targets from various AGN catalogues in the literature (see Sect. 3.4) with the polygons representing the FoVs of all JWST observations. The eJWST interface offers a versatile and user-friendly platform for downloading tables in multiple formats, including VOTable, comma-separated values, and the flexible image transport system. By utilizing these download options, we retrieved the JWST observations through an ADQL query directly on the interface without incurring significant time costs.

After retrieving all JWST observations, we cross-matched them with the target coordinates from the AGN catalogues using TOPCAT's (Taylor 2005) `inSkyPolygon` function, to check if the coordinates fell within any polygon (see Fig. 4). TOPCAT's `inSkyPolygon` tool provides a practical approach for spatial querying within a specified polygonal region of the sky. The immediate and interactive nature of `inSkyPolygon` is particularly useful when dealing with large datasets that need filtering based on spatial location.

A similar approach is offered by the eJWST interface directly, using ADQL queries (see Listing 1). Here, an intersect function is used to verify if a circle with a certain radius around the target coordinates lies within the polygon. For the matching procedure, we did not want to use a search radius around the AGN coordinates to avoid imposing arbitrary constraints, such as defining the matching area as a fraction of the FoV, or deciding which coordinates to prioritize. Also, this could cause false

target_keywords
SREGION=POLYGON ICRS 53.048538679 -27.783081982 53.049154399 -27.783081982 53.049154399 -27.783081982
SREGION=POLYGON ICRS 53.148412135 -27.782344591 53.1486656356 -27.782344591 53.1486656356 -27.782344591
TARGCAT=Clusters of Galaxies|TARGDESC=Abell clusters|TARGET_DESCRIP=Clusters of Galaxies; Abell clusters
SREGION=POLYGON ICRS 150.2329608305 2.30823519041 150.26638001444 2.29541644804 150.233538001
SREGION=POLYGON ICRS 53.133518002 -27.845339103 53.133710681 -27.845339103 53.133710681 -27.845339103
SREGION=POLYGON ICRS 257.929488855 11.140882224 257.944270455 11.130547374 257.954813774 11.130547374

Fig. 1. Snippet of target_keywords with the category and description label highlighted.

³ <https://www.stsci.edu/scientific-community/software/astronomers-proposal-tool-apt>

⁴ <https://jwst-docs.stsci.edu/jppom/targets/fixed-targets/target-descriptions#qsc.tab=0>

⁵ <https://www.stsci.edu/jwst/science-execution/approved-programs>

Listing 1. ADQL query for cross-match.

```
SELECT *
FROM jwst.archive
WHERE ((jwst.archive.calibrationlevel = 3) OR (jwst.archive.calibrationlevel = -1))
AND (position_bounds_spoly IS NOT NULL
AND INTERSECTS(CIRCLE('ICRS',ra,dec,0),position_bounds_spoly)=1)
```

positives in regions close to the edges of the FoV. Thus, we carried out a cross-match to pixel coordinates instead of the radius search. To do this in the eJWST, we set the radius to 0. This yields the same result as the `inSkyPolygon` function but, due to its being dependent on the database server load, filtering large datasets (such as those with ≥ 600 entries) can be computationally expensive and time-consuming. Therefore, the on-the-fly filtering of `inSkyPolygon` aligned better with our requirements for fast and efficient data analysis in this context.

3.4. Catalogues

To identify AGNs outside of the JWST proposals, we utilized the following key catalogues and literature sources to ensure comprehensive coverage and accuracy. The main properties of all catalogues used can also be found in Table B.1.

- The Million Quasar (Milliquas) catalogue by [Flesch \(2023\)](#) includes all published quasars up to June 30, 2023, featuring 907,144 type-I quasi-stellar objects and AGNs, 66,026 high-confidence radio/X-ray associated candidates, and 48,630 type-II and BL Lac objects, totaling 1,021,800 entries. Continuously updated since 2009, the catalogue maintains records from various sources, including data from the Dark Energy Spectroscopic Instrument (DESI), the Sloan Digital Sky Survey Data Release 18 (SDSS-DR18), the Second XMM-Newton Serendipitous Source Catalogue (2XMM-Newton), the Cosmic Evolution Survey (COSMOS), the Wide-field Infrared Survey Explorer (WISE), the 2dF, the Six-degree Field Galaxy Survey (6dF), and the Two Micron All Sky Survey (2MASS). By cross-matching the Milliquas catalogue with all JWST observations, we find 2,495 AGNs from the Milliquas catalogue in one or more JWST observations.
- The SDSS MaNGA AGN (MaNGA) catalogue by [Comerford et al. \(2024\)](#) identifies AGNs in the final DR17 MaNGA sample of approximately 10,000 nearby galaxies using mid-infrared, X-ray, and radio data, alongside broad emission lines in SDSS spectra. They used data from the Wide-field Infrared Survey Explorer (WISE), the Burst Alert Telescope (BAT), the NRAO VLA Sky Survey (NVSS), and the Faint Images of the Radio Sky at Twenty Centimeters (FIRST), applying selection criteria in these wavelengths, and identified a total of 397 AGNs. The cross-matching resulted in multiple JWST observations for 7 of these AGNs.
- The eROSITA Final Equatorial Depth Survey (eFEDS) by [Liu et al. \(2022\)](#) is one of the largest contiguous-field X-ray surveys observing a total area of 142 deg^2 . It provides a comprehensive catalogue of X-ray sources with extensive multi-band photometric and spectroscopic coverage. The eFEDS AGN catalogue includes 22,079 AGNs from the 27,910 sources found by the main X-ray catalogue, predominantly featuring X-ray unobscured AGNs. The cross-matching found 8 of them in JWST observations.

- The Stripe 82X survey (Stripe) multi-wavelength catalogue by [Ananna et al. \(2019\)](#) covers 31.3 deg^2 using *Chandra* and *XMM-Newton*. The updated catalogue includes 5,961 X-ray sources with multi-wavelength counterparts providing spectroscopic and photometric redshifts. We selected for our sample all objects listed as Type 1 and Type 2 AGNs, as well as quasi-stellar objects (QSOs), which resulted in a total of 2,459 AGNs. From these, 27 were found in JWST observations.
- The CDFS: 7 Ms Source catalogues ([Luo et al. 2017](#)) is an X-ray source catalogue covering 484.2 arcmin^2 . The main catalogue includes 1,008 X-ray sources, providing object classification of 711 AGNs with mostly spectroscopic redshifts. Here, 419 of those AGNs were observed by JWST.
- The second data release of the *Swift*/BAT AGN Spectroscopic Survey (BASS) presents a catalogue of AGNs by [Koss et al. \(2022\)](#) along with their optical spectroscopy. This release includes 858 hard-X-ray-selected AGNs from the *Swift*/BAT 70-month sample, updating the previously released catalogue of AGNs by [Baumgartner et al. \(2013\)](#). Using instruments like Very Large Telescope (VLT)/X-shooter and Palomar/Doublespec they offer high-resolution spectra and broad wavelength coverage (3200–10,000 Å). This release is notable for its completeness in spectroscopic coverage (100% for AGNs), with nearly all AGNs having spectroscopic redshift measurements (99.8%). We found 61 of them in JWST observations.
- The catalogue of quasars and active nuclei: 13th edition (Veroncat), published by [Véron-Cetty & Véron \(2010\)](#), is the follow-up of the previously published catalogues ([Véron-Cetty & Véron 2006, 2003](#)). This edition primarily uses the fifth, sixth, and seventh data releases from the SDSS [Adelman-McCarthy et al. \(2007, 2008\)](#); [Abazajian et al. \(2009\)](#), presenting a compilation of 133,336 quasars, 1,374 BL Lac objects, and 34,231 active galaxies, including 16,517 Seyfert 1s. They include measured redshifts known before July 1, 2009, and positions. We made use of their AGN table (34,231 objects), which lists ‘active galaxies’ such as Seyfert 1s (S1), Seyfert 2s (S2), and Low-Ionization Nuclear Emission-line Regions (LINERs) as defined by [Heckman \(1980\)](#). In total 399 of these AGNs were found in JWST observations.
- The ROSAT-FIRST AGN catalogue (Rosat) by [Brinkmann et al. \(2000\)](#), combines data from the ROSAT All-Sky Survey (RASS) and the Very Large Array (VLA) FIRST 20cm survey, focusing on 843 X-ray sources with unique radio counterparts. The catalogue uses RASS for X-ray data and FIRST for high-sensitivity radio data (1 mJy at 1.4 GHz) with accurate positioning (about 1 arcsecond). In total 294 confirmed AGNs are identified. Here, 5 AGNs were found in JWST observations.
- The *Gaia*-Celestial Reference Frame 3 (*Gaia*-CRF3) ([Gaia Collaboration et al. 2022](#)) filters QSO/quasar targets from the *Gaia* Data Release 3 (*Gaia* DR3) with over 90% purity. The *Gaia*-CRF3 content lists QSO-like sources re-

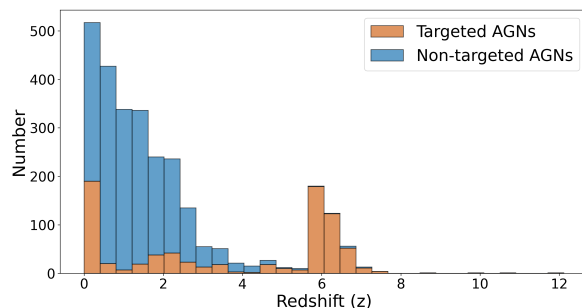


Fig. 2. Histogram of redshifts in the eJWST AGN catalogue. See text for details.

trieved from 17 external catalogues, for example the All Wide-field Infrared Survey Explorer (AllWISE) (Sereš et al. 2015), Milliquas v6.5 (Flesch 2015), R90 (Assef et al. 2018), the Fifth Large Quasar Astrometric Catalog (LQAC-5) (Souchay et al. 2019), and more. Accessing the `gaiadr3.qso_candidates` table via the *Gaia* archive⁶, we obtained a dataset that contains extragalactic sources but has low purity due to a completeness-driven selection. To then select the *Gaia*-CRF3 targets, we applied the criterion `gaia_crf_source = 'True'`, which retrieves all 1,614,173 sources from the CRF3 table. To align with the JWST coordinates epoch, we directly transformed the given coordinates from the J2016 to the J2000 epoch using the *Gaia* archive’s `ESDC_EPOCH_PROP` function. In total 400 AGNs were found in one or several JWST observations.

- The local *Swift*/BAT AGN (Swiftbat) study provides a list of 277 local hosts of selected AGNs from the 58-month *Swift*/BAT AGN sample (Lutz et al. 2018). Covering 14 – 195 keV X-rays they ensure detection of all but the most Compton-thick AGNs, including only $z < 0.06$ objects. The study considers only confidently identified AGNs, excluding low-luminosity AGNs below the BAT detection threshold. The cross-matching revealed that 44 AGNs from this sample were found in one or several JWST observations.

3.5. Redshift retrieval

When redshifts were available in the external catalogues, we extracted and stored them in separate columns for each catalogue, for example ‘z (catalogue name)’. If a catalogue provided both spectroscopic and photometric redshifts, the spectroscopic redshifts were prioritized.

When available, information on the redshift type (spectroscopic or photometric) and the corresponding reference (in the form of a bibcode) was extracted from each catalogue or, when necessary, from the associated catalogue paper. This information was then stored in dedicated columns, for example ‘zType (catalogue name)’. If the catalogue or its description explicitly stated the method used, we assigned the redshift type accordingly (e.g. identification by spectral lines → spectroscopic). If no clear information was available, the type was set to ‘?’ . For catalogues providing their own redshifts (e.g. MaNGA, eFEDs, and Stripe), the bibcode of the corresponding publication was used as reference, whereas for large compilations of literature values (e.g. Milliquas, Véron-Cetty, and Véron), the reference

columns given by the catalogue were used to identify and assign the appropriate bibcodes.

Since many of the targeted AGNs lacked redshift information in either the proposal or catalogue data, we opted to match them with the NASA/IPAC Extragalactic Database (NED). Using the `query_region()` function from the `astroquery.ned` package, we performed a coordinate-based matching procedure with a 1-arcsecond search radius, using the target coordinates provided by eJWST for all objects in our catalogue. This coordinate-based query was used to return the redshift, redshift type and redshift reference from NED. We then compared NED redshifts with catalogue values and removed NED matches when the difference exceeded 0.01. For the remaining reliable matches, the NED results were stored in dedicated columns: `z (NED)`, `zType (NED)`, and `zRef (NED)`. To integrate these results into the working dataset, the NED values were merged into the main redshift (`z`), redshift type (`zType`), and redshift reference (`zRef`) columns wherever available. Redshift types were assigned according to the NED classification scheme, as outlined in their database guide⁷. In cases where no NED entry was returned, we kept the catalogue-provided values according to the following priority order: Milliquas, MaNGA, eFEDs, Stripe, CDFS, BASS, Veroncat, and Rosat. This priority order was established based on the completeness, date of measurement, and accuracy of the information from each source. Missing redshifts were marked as Not a Number (NaN). To maintain transparency, we introduced a ‘zNED’ flag. Entries with NED-derived redshifts are marked with ‘y’, while those with catalogue-based values are marked with ‘n’. This framework ensures that catalogue redshifts are preserved while NED information is systematically incorporated and clearly identified.

In total we found and list redshifts for 86.78% (2,814) of all individual AGNs (3,242) in our catalogue. A distribution of the redshift for all AGNs (targeted and non-targeted) can be found in Fig. 2.

3.6. Object type retrieval

For the targeted AGNs, the object classifications were retrieved directly from the descriptions provided by the proposers. For the non-targeted AGNs, we extracted the object types from the external catalogues whenever available. These catalogues differ in how they report AGN subclasses. For example, Veroncat distinguishes between type-1 and type-2 AGNs, and intermediate subclasses such as S1.0–S1.9 for intermediate Seyferts, S2 and S2? for confirmed and probable type-2 AGNs, S3 for LINERs, and BL for confirmed BL Lacs. While BASS specifies Seyfert subclasses (e.g. Sy1, Sy1.9, and Sy2) and additionally distinguishes beamed AGN types such as blazars (BZQ, BZG, and BZB). To avoid ambiguity, we did not directly adopt catalogue abbreviations, since identical codes are sometimes used with different meanings across catalogues (e.g. ‘S’ denoting either ‘Seyfert’ or ‘Star’). Instead, we constructed a harmonized classification scheme based on the catalogue descriptions, writing out the types as clearly as possible while retaining minimal abbreviations. For example, the Milliquas classification ‘A = AGN, type-I Seyferts/host-dominated’ was recast as ‘AGN type-1’, and ‘K = NLQSO, type-II narrow-line core-dominated’ was listed as ‘QSO-NL’. Where available, we also incorporated information on whether the source is narrow-line (NL) or broad-line (BL). A ‘?’ was added to object types to indicate uncertain classifications

⁶ <https://gea.esac.esa.int/archive/>

⁷ <https://ned.ipac.caltech.edu/Documents/Guides/Database>

(e.g. ‘AGN-BL?’), ‘?’ for highly questionable assignments, and a single ‘?’ (with no object type specification) was used for completely unknown types. Additional refinements were applied to preserve catalogue-specific information, such as ‘-b’ in Veroncat for broad Balmer lines, ‘-h’ for polarized Balmer lines, and ‘-i’ for broad Paschen lines observed in the infrared. A full description of the original classifications and the mapping is provided in Tables A.1–A.6.

3.7. Identifying duplicates

After the cross-matching process, results from each catalogue were combined into a single data frame using an outer merge (which returns all the rows from both data frames, with NaN for any missing matches) on the ‘observationid’. This groups all objects identified within the same FoV of observation together, regardless of whether they were the same objects. These groups were then analysed to identify cases where the same object was listed in multiple catalogues, ensuring that duplicates were not included. Our approach involved two steps: first, a redshift-based coordinate cross-match between all targets found within the same observation. Using the redshift data provided by the catalogues, we calculated an appropriate matching radius by determining the angular separation in arcseconds that corresponds to a proper kiloparsec at the given redshift z for each object:

$$\theta_{\text{arcsec}} = \frac{x_{\text{kpc}}}{D_A}, \text{ where } D_A = \frac{S_k(r)}{1+z}. \quad (1)$$

Here θ_{arcsec} is the angular separation in arcsec, x_{kpc} the physical size of the object in kpc, D_A the angular diameter distance, z the redshift, and $S_k(r)$ the Friedmann–Lemaître–Robertson–Walker metric. We made use of the `arcsec_per_kpc_proper(z)` function from the `astropy.cosmology.funcs` module to determine $1/D_A$. The physical size was set to 1 kpc to ensure that only objects with very close angular positions are considered as the same. This leverages the high positional accuracy typically reported in the catalogues as well as taking into account the considerable fraction (14.35%) of objects of redshifts between 5 and 8 (see Fig. 2). Since galaxy sizes generally decrease with increasing redshift (van der Wel et al. 2014; Whitney et al. 2019; Costantin et al. 2023; Ormerod et al. 2024), a threshold of 1 kpc is reasonable. For example, Whitney et al. (2019) found that galaxies at $z = 7$ have a median size of 1.64 kpc. The matches identified by this procedure were manually inspected, with particular attention to the redshifts (when available) to ensure the objects were not mistakenly matched due to projection effects. Secondly, we compared the given names of the AGNs, along with their redshifts, for the objects not previously found as matches. If the name (excluding spaces and hyphens ‘-’) and the provided redshift were identical, the targets were considered the same. Each identified match was then subject to additional manual inspection, including verification against databases such as NED. All objects without redshift information were also manually inspected, and, when possible, matches were verified through the use of NED. Only targets identified with high certainty as matches were noted as such; otherwise, they were retained as individual targets.

After this matching procedure, we now count a total of 3,242 unique AGNs in our catalogue. With a total of 968 targeted and 2,274 non-targeted AGNs. Individual AGNs were counted by coordinates with a matching radius of 1 arcsecond. This counting method is kept throughout the work. For matches with the largest

separation (>0.5 arcsec) individual checks were done and possible miscounted objects were corrected.

3.8. Background observations

We provide information on whether the main goal of an observation was science, calibration, or background. Data intended for science and calibration were filtered using the ‘Intend’ keyword from the archive. To identify background data, we filtered by instrument keyword `bkgdtarg` = `t(rue)`.

We also searched for the `TARGNAME` keyword in the `target_keywords` for specific descriptors identifying background observations, such as ‘background’, ‘BCKGND’, ‘Background’, and more. Observations with these descriptors were then labelled as background observations. Some targets were not explicitly labelled as background by such keywords but were identified as such by their target names. To address this, we conducted a further check for any names containing terms suggestive of background observations (e.g. NGC 6552-Background). All observations identified as background through this process were marked accordingly with the entry ‘Background’ in the intent column. In total 1,150 observations were marked as background.

4. Caveats

4.1. Accuracy of the (cross-)matching

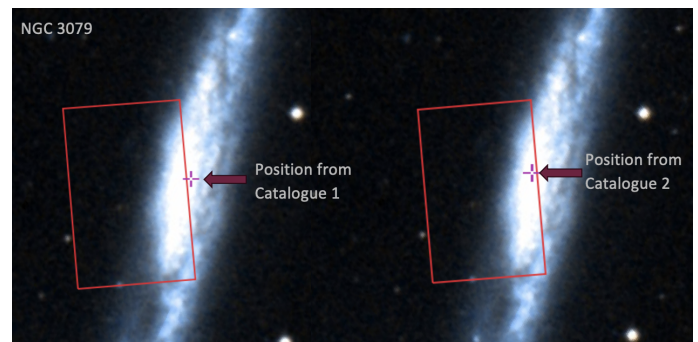


Fig. 3. Optical DSS2 image from ESASky of NGC 3079 showing its coordinates (purple cross) according to Swiftbat (left panel) and Milliquas (right panel), and the FoV of observation `jw05627017002_xx102_00002_miri` (red rectangle). NGC 3079 appears in our catalogue with the Milliquas coordinates.

The astrometric accuracy of each AGN catalogue (Sect. 3.4) varies depending on the telescopes used, their resolution, survey epochs, and methodologies used to determine the coordinates of each source. The uncertainties in the coordinates vary not only between catalogues, but sometimes also within a catalogue. Most catalogues report their accuracy for the coordinates for their sources, for example less than 2'' for CDFS, Rosat, Stripe, and *Gaia*, or a few milliarcseconds for MaNGA. Some catalogues, especially the largest ones, make it particularly challenging to determine the uncertainty of the source coordinates (e.g. Milliquas; see Flesch 2023, for details). This causes some sources to have slightly different coordinates in different catalogues, even after adjusting all the coordinates to J2000.0.

Thus, during the coordinate cross-matching process to create our catalogue, some targets may be inside an observation’s FoV or outside the FoV depending on the reference catalogue used for the coordinates. These targets are included in our catalogue, but

Table 2. Example of matches found via redshift-dependent cross-match for the same observation in two catalogues.

Milliquas Name	Veroncat Name	RA (Milliquas)	Dec (Milliquas)	RA (Veroncat)	Dec (Veroncat)	observationid
Q J12367+6215	Q J12367+6215	189.175967	62.262648	189.175833	62.262500	jw01181-c1009_s03562_nirspec_f290lp-g395m
BX 1335	BX 1335	189.186667	62.258611	189.186250	62.258611	jw01181-c1009_s03562_nirspec_f290lp-g395m
Q 1234+6231	NaN	189.095554	62.257402	NaN	NaN	jw01181-c1009_s03562_nirspec_f290lp-g395m
A03.161	NaN	189.122696	62.253620	NaN	NaN	jw01181-c1009_s03562_nirspec_f290lp-g395m
HETDEX 2970	NaN	189.194290	62.246147	NaN	NaN	jw01181-c1009_s03562_nirspec_f290lp-g395m
NaN	B2.161	NaN	NaN	189.122500	62.253611	jw01181-c1009_s03562_nirspec_f290lp-g395m

they will appear listed only under the reference catalogue, and the coordinates that fall inside the FoV. An example is shown in Fig. 3 of an MIRI/IMAGE observation (FoV size $74'' \times 113''$; see Table 4), of the target NGC 3079. The target coordinates from the Milliquas catalogue (RA = 150.493889, Dec = 55.680556) are inside the observation FoV, whereas the target coordinates from the Swiftbat catalogue (RA = 150.4905, Dec = 55.6799) fall outside. In this case, NGC 3079 will appear in our catalogue with the Milliquas coordinates.

4.2. Extended sources

The AGN coordinates in the reference catalogues are usually given for the nucleus of the source. Thus, some observations of extended AGN hosts may be excluded from our catalogue, as the nucleus of the galaxy may not be within the observation FoV (e.g. observations mapping the star formation in the outer regions of an AGN host galaxy, where the galactic nucleus is not included). This was mostly found for nearby objects, since here the resolution enables observations targeting specific parts of the galaxy. We are confident that this issue only affects a small part of the AGN observations, since most of these region-specific observations of an AGN-hosting galaxy are targeted observations, and thus most likely labelled as an AGN by the proposer. Furthermore, most of these observations will include a pointing including the nucleus. Therefore, we expect most, if not all, of these targets to be included in our targeted sample.

4.3. Masking in the FoV

The polygons describing the observations FoV provided by CAOM cover the whole FoV of the instrument, including regions that may be masked by hardware, bad pixels, etc. Thus, there could be sources included in our catalogue that fall within the observations FoV, but coincide with one of these areas (see Fig. 4).

Currently, we need to locate and remove those observations manually, so there will be cases included in the catalogue. Addressing these, and finding a suitable approach is part of future improvements of our catalogue.

4.4. Planned observations

Our catalogue includes both observed and planned JWST observations where AGNs fall within the data FoV. Over time, especially for proposed observations or pipeline reprocessing, some data details may change. New versions of the catalogue will account for those changes.

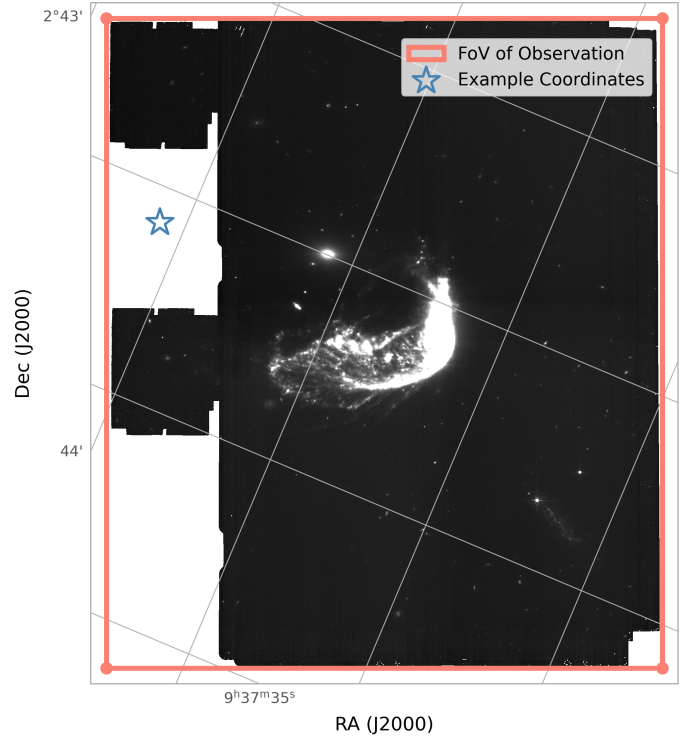


Fig. 4. Example of an AGN with coordinates inside the FoV of an observation but in a masked area of the data. This MIRI image of the Penguin Galaxy (NGC 2936) corresponds to observation ID jw06564-o001_t001_miri_f770w. The coloured rectangle shows the FoV as obtained from the position_bound_spoly keyword. The blue star shows an example of coordinates that fall within the FoV but lack data due to masking (in this case caused by the MIRI coronagraphs).

5. AGN surveys and little red dots

5.1. On-going AGN surveys

JWST has enabled a wide range of observational surveys, many of which are expected to uncover new AGNs. These programmes span diverse objectives, through extragalactic surveys and targeted investigations covering different types of sources, from the local to the distant Universe.

Extragalactic surveys such as the JWST Advanced Deep Extragalactic Survey (JADES) (PIDs 1180, 1181, 1210, 1286 1895, 1963, 3215, [Eisenstein et al. 2023](#)), the Cosmic Evolution Early Release Science Survey (CEERS) (PID 1345, [Finkelstein et al. 2017](#)), and the Systematic Mid-infrared Instrument (MIRI) Legacy Extragalactic Survey (SMILES) (PID 1207; [Rieke et al. 2024](#)) are designed to explore the high-redshift Universe and are expected to discover many high-redshift AGNs. Targeted programmes such as FRESCO (PID 1895; [Oesch et al. 2021](#)) and COSMOS-Web (PID 1727; [Casey et al. 2023](#)) concentrate on specific regions of the sky, with FRESCO observing the GOODS

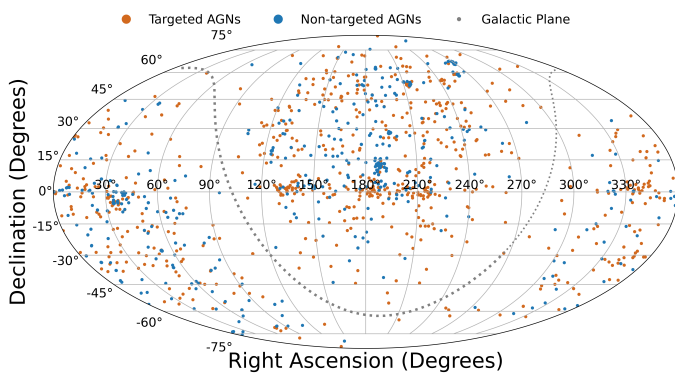


Fig. 5. AGNs in the catalogue. This plot includes targeted and non-targeted AGNs in a Mollweide projection. Orange and blue dots mark the coordinates of targeted and non-targeted AGNs (respectively) included in the catalogue. The dotted line follows the Galactic plane in the sky.

legacy fields and COSMOS-Web extending studies of the COSMOS field. The AGNs discovered by these and other similar JWST programmes have been reported in several studies (Kocevski et al. 2023; Scholtz et al. 2025; Larson et al. 2023; Carniani et al. 2024; Matthee et al. 2024; Maiolino et al. 2024; Übler et al. 2024; Kocevski et al. 2025; Lyu et al. 2024; Juodžbalis et al. 2024).

In addition to large-scale extragalactic efforts, JWST programmes also investigate AGNs in the local and intermediate-redshift Universe. Notable examples include the ERS Q3D programme (PIDs 1335 and 3807; [Wylezalek et al. 2022](#); [Bertemes et al. 2025](#)) and GATOS (PIDs 1670, 2064, 4225, 3535, 4892, 5017, 7195, 7802, and 7429; [García-Bernete et al. 2024a,b](#); [Zhang et al. 2024](#)), as well as studies targeting (ultra-)luminous infrared galaxies, for example programmes such as PIDs 1204 and 3368, GOALS ([Rich et al. 2023](#)), and individual work by [Huang et al. \(2023\)](#) and [Dan et al. \(2025\)](#). These objects, among the brightest in the local Universe, often host heavily obscured AGNs.

Most of these surveys are ongoing and collecting or analysing data; therefore, their discoveries of AGNs are still in progress. Some publications have already listed AGNs or AGN candidates identified in the above-mentioned surveys (e.g. AGNs found in SMILES using the MIRI instrument; [Lyu et al. 2024](#)). However, due to the ongoing nature of these programmes, we decided not to include such listings until more complete catalogues are published. Some AGNs from these surveys are included in our catalogue, if their JWST observations were labelled as AGNs in the proposal or if matches were found in the catalogues used for cross-matching. For example, observations from the JADES survey under PIDs 1180 and 1181 were not explicitly labelled as AGNs but were included in our catalogue through the cross-matching process. In contrast, PID 1670 from the GATOS programme provided explicit AGN labels for their observations, and thus they were categorized as targeted observations in our catalogue. This approach is consistent across the other listed surveys.

In the future, as survey-specific AGN catalogues become available, we plan to incorporate them into ours following the same methodology described above.

5.2. Little red dots

With the beginning of JWST observations, previously hidden objects have been uncovered. Among these discoveries, there is a

new population of compact, red galaxies identified in the first observations of the JWST CEERS programme (Yang et al. 2023; Labb   et al. 2023), known as little red dots (LRDs). These galaxies are characterized by their bimodal spectral energy distributions, exhibiting both a Lyman break and a Balmer break (Labb   et al. 2023; Barro et al. 2024). The classification of LRDs remains an open question, with ongoing debates about whether they should be categorized as AGNs (Barro et al. 2024; Matthee et al. 2024; Kocevski et al. 2025; Akins et al. 2025). Some studies suggest that the spectral energy distributions of LRDs are consistent with significant AGN contributions (Durodola et al. 2025), and the detection of very broad Balmer emission lines (Greene et al. 2024) further supports this interpretation. However, other reports highlight properties of LRDs that are difficult to explain with an AGN classification. For instance, the absence of X-ray detections (Yue et al. 2024; Ananna et al. 2024; Kokubo & Harikane 2025) and the lack of variability (Kokubo & Harikane 2025), both typically associated with AGNs, challenge this scenario. Additionally, studies show that for some LRDs the broad-line signatures are found to be in agreement with behaviour found in galaxies that do not host an AGN (Baggen et al. 2024; Kokubo & Harikane 2025; P  rez-Gonz  lez et al. 2024).

Because these objects are relatively new, they are not included in the external catalogues we used, and the eJWST proposals do not provide a dedicated LRD keyword. Collecting all currently published LRDs without an existing comprehensive catalogue is beyond the scope of the present work. Therefore, we have not included LRDs in our catalogue. However, if future research provides a comprehensive catalogue of these objects, we will incorporate them into our sample and flag them as AGN candidates when a consensus on the nature of these sources is reached.

6. Catalogue description

Our catalogue contains 3,242 AGNs (968 targeted AGNs and 2,274 non-targeted AGNs), observed in a total of 360,260 calibration level 3 (science-ready) observations plus 47,650 planned observations (including those from Cycle 4 proposals). Among the level 3 observations, 267,219 are public, while 93,041 remain private. Breaking down the observation types for the level 3 observations, 329,425 are classified as science, 1,000 as background, and 1,540 as calibration observations.

The catalogue is structured as a comma-separated value table and includes various columns: Name, Coordinates (RA and Dec), ObjType, Ref, z, zType, zRef, zNED, Observation ID, Instrument, Aperture, Exptype, Filter, Calibration Level, Exptime, Public, Proposal ID, Release Date, Intent, Central Wavelength, Targeted, Data Link, Proposal ID Link, TSOVISIT, eJWST Name, and eJWST Coordinates, as well as Name, ID, z, zType, zRef, and objType for all external catalogues used (see Tables C.1 and C.2). For each AGN, the catalogue lists the Observation ID corresponding to different observations identified through our cross-matching procedure, along with object names. These names may be sourced from the external catalogues, JWST proposals, or generated from the J2000 coordinates. The coordinates are provided in degrees (J2000). Additionally, the catalogue includes direct download links for data files (when publicly available) as well as links to the original proposals. We include a flag indicating which sources have time-series observations (TSOs) with JWST, as reported in the JWST archive via the TSOVISIT keyword. Sources reported as TSOs are flagged with ‘t’, while those reported as non-TSOs are marked with ‘n’. Sources without a TSOVISIT entry in the archive are marked as ‘NaN’.

Table 3. Comparison of the number of all observations of every AGN per instrument mode in the catalogue.

Instrument	Targeted	Non-Targeted	FoV (arcsec)
NIRCAM			
GRISM	17,183	160,204	129×129
IMAGE	1,015	34,430	$2 \times 132 \times 132$
CORON	0	4	20×20
TARGACQ	0	2	
MIRI			
IFU	2,112	485	3.7×3.7 to 7.7×7.7
IMAGE	1,430	8,310	74×113
SLIT	103	11	0.51×4.7
NIRISS			
WFSS	408	97,085	133×133
IMAGE	89	520	133×133
AMI	15	27	5.2×5.2
NIRSpec			
IFU	2,047	172	3.0×3.0
SLIT	688	7	0.2×3.2 , 0.4×3.65 , 1.6×1.6
MSA	28	81,559	216×204
FGS			
FGS1	0	2	138×138
FGS2	0	1	138×138

Table 4. *

This table includes both science-ready and planned observations. Notice that individual AGNs can have multiple observations. The table also includes the FoV in arcseconds and the point spread function (PSF) full width at half maximum (FWHM) in arcseconds for each instrument observing mode. For the NIRSpec Microshutter Array (MSA) FoV, the dimensions represent the individual shutter size in the dispersion direction and spatial direction. The PSF FWHM values reflect a range due to their dependence on the different filters and channels used.

We note that this catalogue does not determine or analyse whether an observation is a TSO, it simply reports the information provided by the eJWST archives. In addition, we incorporated the matches from the external catalogues, preserving the name, coordinates, and redshift columns for each catalogue used. As a result, if a target appears in multiple external catalogues, this will be reflected in the corresponding columns for those catalogues. A full description of all columns can be found in Table C.1.

We list redshift information for a total of 2,814 AGNs, taken from either the external catalogues (for non-targeted AGNs) or NED (for targeted and non-targeted AGNs). We show the redshift distribution of all targets in the catalogue in Fig. 2. We notice that the non-targeted AGNs predominantly have redshifts below $z = 3$, possibly reflecting the observational limits of previous telescopes. In contrast, the targeted AGNs tend to be higher-redshift sources, highlighting the current interest in early Universe AGNs and showcasing JWST’s capabilities to observe them.

Table 4 compares the distribution of AGNs in the catalogue per instrument and observing mode. Most observations correspond to the NIRCam/GRISM mode, for both targeted and non-targeted AGNs. Additionally, for targeted AGNs, there is a substantial number of IFU observations (MIRI and NIRSpec). This preference likely stems from the unique advantages of IFUs in providing spatially resolved spectral information. In contrast, a significant number of non-targeted AGNs have been identified using the NIRISS/WFSS and NIRSpec/Microshutter Array instruments. This is probably due to their large FoVs, which allow them to include more sources in their observations.

In Fig. 5 we present the sky distribution of all targeted and non-targeted AGNs from our study using a Mollweide projection. The broad distribution of positions demonstrates that our external catalogue search did not preferentially focus on specific regions of the sky. It also highlights how the observing programmes tend to avoid the galactic plane, as expected.

7. Conclusion

In this work we present a catalogue of all AGNs observed with JWST, whether as direct targets or serendipitous observations in the FoV of any dataset, complete by March 20 2025, right after the publication of the Cycle 4 results. The catalogue lists observations of 3,242 individual AGNs. For the targeted AGNs, we applied two distinct selection approaches. First, we used ADQL queries to filter AGN observations by specific keywords designated by the proposers. Second, we manually reviewed relevant JWST programme proposals to identify additional targeted AGNs. This combined approach resulted in the identification of 968 individual targeted AGNs. For the non-targeted AGNs, we identified objects located within the JWST FoV by cross-matching multiple external AGN catalogues with JWST observations, ensuring that duplicate entries were systematically removed when necessary. In total, 2,274 non-targeted AGNs were identified through this process.

Observations of nearby or extended hosts of AGNs may be underrepresented in our catalogue if the FoV of any observations does not include the nuclear region, as the catalogues used for the cross-correlation typically give the coordinates of the nucleus. We expect such omissions to be minimal, as close-up ob-

servations of AGN hosts are likely captured by our targeted AGN selection. Additionally, it is possible that an AGN falls within the FoV of an observation but lies in a masked region of the instrument, resulting in no usable data for that target. Currently, we are working on automatizing a comprehensive method for accounting for these cases, as well as the (currently manual) proposal review process to identify targeted AGNs.

For future releases, we aim to update the catalogue at least once a year to include new observed and planned data, and incorporate additional AGN catalogues and surveys, as well as LRDs and potentially new sources, as data become available.

Data availability

The last update of our catalogue, at the time of writing, was completed on March 20, 2025, to include the Cycle 4 approved proposals. As the archives are constantly updated with new data, we aim to update our catalogue on an — at least — yearly basis, in time for every JWST call for proposals.

Code for this study and the latest version of the catalogue is available at GitHub⁸. The catalogue presented in this work (Table C.2) is available in electronic form at the CDS via anonymous FTP (<ftp://cdsarc.u-strasbg.fr>) or via <http://cdsweb.u-strasbg.fr/cgi-bin/qcat?J/A+A/>.

Acknowledgements. We thank the referee for their suggestions that helped improve the catalogue and the paper. VL thanks the SCI-S Trainee Programme of the European Space Agency (ESA) for providing me with the incredible opportunity to work on this project. The support and resources provided by the program were instrumental in the successful completion of this work. Additional thanks to M. Arévalo and J. Espinosa for their valuable assistance in navigating the eJWST archive and their guidance to CAOM. CC acknowledges support from the ESA Fellowship in Space Science program. AL acknowledges support from ESA through the ESA Space Science Faculty support programs. AAH acknowledges support from grant PID2021-124665NB-I00 funded by the Spanish Ministry of Science and Innovation and the State Agency of Research MCIN/AEI/10.13039/501100011033 and ERDF A way of making Europe. The authors thank AGN group at ESAC, and its visitors, for useful scientific discussions and feedback on how to improve the catalogue and source selection. This research has made use of NASA’s Astrophysics Data System Bibliographic Services, and of the NASA/IPAC Extragalactic Database (NED), which is operated by the Jet Propulsion Laboratory, California Institute of Technology, under contract with the National Aeronautics and Space Administration. This research has made use of the Spanish Virtual Observatory (<https://svo.cab.inta-csic.es>) project funded by MCIN/AEI/10.13039/501100011033/ through grant PID2020-112949GB-I00. This work is based on observations made with the NASA/ESA/CSA *James Webb* Space Telescope. The data were obtained from the [European JWST archive \(eJWST\)](#), which is operated by the European Space Agency; and the Mikulski Archive for Space Telescopes at the Space Telescope Science Institute, which is operated by the Association of Universities for Research in Astronomy, Inc., under NASA contract NAS 5-03127 for JWST.

References

Abazajian, K., Adelman-McCarthy, J. K., Agüeros, M. A., et al. 2003, AJ, 126, 2081

Abazajian, K. N., Adelman-McCarthy, J. K., Agüeros, M. A., et al. 2009, ApJS, 182, 543

Adelman-McCarthy, J. K., Agüeros, M. A., Allam, S. S., et al. 2008, ApJS, 175, 297

Adelman-McCarthy, J. K., Agüeros, M. A., Allam, S. S., et al. 2007, ApJS, 172, 634

Akins, H. B., Casey, C. M., Lambrides, E., et al. 2025, ApJ, 991, 37

Ananna, T. T., Bogdán, Á., Kovács, O. E., Natarajan, P., & Hickox, R. C. 2024, ApJ, 969, L18

Ananna, T. T., Salvato, M., Lamassa, S., et al. 2019, VizieR Online Data Catalog: Stripe 82X survey multiwavelength catalog (Ananna+, 2017), VizieR On-line Data Catalog: J/ApJ/850/66. Originally published in: 2017ApJ...850...66A

Arevalo, M., Espinosa, J., Marston, A., et al. 2024, in ASPCS, Vol. 535, Astronomical Data Analysis Software and Systems XXXI, ed. B. V. Hugo, R. Van Rooyen, & O. M. Smirnov, 247

Assef, R. J., Stern, D., Noiro, G., et al. 2018, ApJS, 234, 23

Baggen, J. F. W., van Dokkum, P., Brammer, G., et al. 2024, ApJ, 977, L13

Barro, G., Pérez-González, P. G., Kocevski, D. D., et al. 2024, ApJ, 963, 128

Baumgartner, W. H., Tueller, J., Markwardt, C. B., et al. 2013, ApJS, 207, 19

Bertemes, C., Wylezalek, D., Rupke, D. S. N., et al. 2025, A&A, 693, A176

Böker, T., Beck, T. L., Birkmann, S. M., et al. 2023, PASP, 135, 038001

Brinkmann, W., Laurent-Muehleisen, S. A., Voges, W., et al. 2000, A&A, 356, 445

Bushouse, H. 2020, in ASPCS, Vol. 527, Astronomical Data Analysis Software and Systems XXIX, ed. R. Pizzo, E. R. Deul, J. D. Mol, J. de Plaa, & H. Verkouter, 583

Bushouse, H., Eisenhamer, J., Dencheva, N., et al. 2024, JWST Calibration Pipeline

Carniani, S., Venturi, G., Parlanti, E., et al. 2024, A&A, 685, A99

Casey, C. M., Kartaltepe, J. S., Drakos, N. E., et al. 2023, ApJ, 954, 31

Circosta, C., Mainieri, V., Lamperti, I., et al. 2021, A&A, 646, A96

Comerford, J. M., Nevin, R., Negus, J., et al. 2024, ApJ, 963, 53

Costantin, L., Pérez-González, P. G., Vega-Ferrero, J., et al. 2023, ApJ, 946, 71

Cresci, G. & Maiolino, R. 2018, Nature Astronomy, 2, 179

Croom, S. M., Smith, R. J., Boyle, B. J., et al. 2001, MNRAS, 322, L29

Dan, K. Y., Seebeck, J., Veilleux, S., et al. 2025, ApJ, 979, 68

Dowler, P. 2012, in ASPCS, Vol. 461, Astronomical Data Analysis Software and Systems XXI, ed. P. Ballester, D. Egret, & N. P. F. Lorente, 339

Dowler, P., Rixon, G., Tody, D., & Demleitner, M. 2019, Table Access Protocol Version 1.1, IVOA Recommendation 27 September 2019

Doyon, R. 2012, in Proceedings of the SPIE, Vol. 8442, Space Telescopes and Instrumentation 2012: Optical, Infrared, and Millimeter Wave, 84422R

Doyon, R., Willott, C. J., Hutchings, J. B., et al. 2023, PASP, 135, 098001

Durodola, E., Pacucci, F., & Hickox, R. C. 2025, ApJ, 985, 169

Eisenstein, D. J., Willott, C., Alberts, S., et al. 2023, submitted to ApJ, arXiv:2306.02465

Ferruit, P. 2012, in Proceedings of the SPIE, Vol. 8442, Space Telescopes and Instrumentation 2012: Optical, Infrared, and Millimeter Wave, 84422O

Finkelstein, S. L., Dickinson, M., Ferguson, H. C., et al. 2017, The Cosmic Evolution Early Release Science (CEERS) Survey, JWST Proposal ID 1345. Cycle 0 Early Release Science

Flesch, E. W. 2015, PASA, 32, e010

Flesch, E. W. 2023, The Open Journal of Astrophysics, 6, 49

Gaia Collaboration, Bailer-Jones, C. A. L., Teyssier, D., et al. 2023, A&A, 674, A41

Gaia Collaboration, Klioner, S. A., Lindegren, L., et al. 2022, A&A, 667, A148

García-Bernete, I., Alonso-Herrero, A., Rigopoulou, D., et al. 2024a, A&A, 681, L7

García-Bernete, I., Rigopoulou, D., Donnan, F. R., et al. 2024b, A&A, 691, A162

Gardner, J. P., Mather, J. C., Abbott, R., et al. 2023, PASP, 135, 068001

Ginsburg, A., Sipőcz, B. M., Brasseur, C. E., et al. 2019, AJ, 157, 98

Graham, A. W., Onken, C. A., Athanassoula, E., & Combes, F. 2011, MNRAS, 412, 2211

Greene, G., Kyprianou, M., Levay, K., et al. 2015, in ASPCS, Vol. 495, Astronomical Data Analysis Software and Systems XXIV (ADASS XXIV), ed. A. R. Taylor & E. Rosolowsky, 77

Greene, J. E., Labbe, I., Goulding, A. D., et al. 2024, ApJ, 964, 39

Harikane, Y., Zhang, Y., Nakajima, K., et al. 2023, ApJ, 959, 39

Harrison, C. M. 2017, Nature Astronomy, 1, 0165

Heckman, T. M. 1980, A&A, 87, 152

Huang, J. S., Li, Z.-J., Cheng, C., et al. 2023, ApJ, 949, 83

Juodžbalis, I., Ji, X., Maiolino, R., et al. 2024, MNRAS, 535, 853

Kocevski, D. D., Finkelstein, S. L., Barro, G., et al. 2025, ApJ, 986, 126

Kocevski, D. D., Onoue, M., Inayoshi, K., et al. 2023, ApJ, 954, L4

Kokubo, M. & Harikane, Y. 2025, ApJ, 995, 24

Kormendy, J. & Ho, L. C. 2013, ARA&A, 51, 511

Koss, M. J., Ricci, C., Trakhtenbrot, B., et al. 2022, ApJS, 261, 2

Labbé, I., van Dokkum, P., Nelson, E., et al. 2023, Nature, 616, 266

Labiano, A., Marston, A., López-Caniego, M., et al. 2023, in Highlights on Spanish Astrophysics XI, ed. M. Manteiga, L. Bellot, P. Benavidez, A. de Lorenzo-Cáceres, M. A. Fuente, M. J. Martínez, M. Vázquez Acosta, & C. Dafonte, 401

Lamassa, S. M., Urry, C. M., Cappelluti, N., et al. 2016, VizieR Online Data Catalog: X-ray Observations of Stripe 82 (LaMassa+, 2016), VizieR On-line Data Catalog: J/ApJ/817/172. Originally published in: 2016ApJ...817..172L

Larson, R. L., Finkelstein, S. L., Kocevski, D. D., et al. 2023, ApJ, 953, L29

Liu, T., Buchner, J., Nandra, K., et al. 2022, A&A, 661, A5

Luo, B., Brandt, W. N., Xue, Y. Q., et al. 2017, ApJS, 228, 2

Lutz, D., Shimizu, T., Davies, R. I., et al. 2018, A&A, 609, A9

Lyu, J., Alberts, S., Rieke, G. H., et al. 2024, ApJ, 966, 229

Maiolino, R., Scholtz, J., Curtis-Lake, E., et al. 2024, A&A, 691, A145

⁸ <https://github.com/VirginiaLenk1/AGNs-in-eJWST.git>

Mantelet, G., Morris, D., Demleitner, M., et al. 2023, Astronomical Data Query Language Version 2.1, IVOA Recommendation 15 December 2023

Matthee, J., Naidu, R. P., Brammer, G., et al. 2024, *ApJ*, 963, 129

Oesch, P., Bouwens, R., Brammer, G., et al. 2021, FRESCO: The First Reionization Epoch Spectroscopic COnplete Survey, JWST Proposal. Cycle 1, ID. #1895

Ormerod, K., Conselice, C. J., Adams, N. J., et al. 2024, *MNRAS*, 527, 6110

pandas development team, T. 2024, *pandas-dev/pandas*: Pandas

Pérez-González, P. G., Barro, G., Rieke, G. H., et al. 2024, *ApJ*, 968, 4

Rich, J., Aalto, S., Evans, A. S., et al. 2023, *ApJ*, 944, L50

Rieke, G. H. 2015, *PASP*, 127, 584

Rieke, G. H., Alberts, S., Shavaei, I., et al. 2024, *ApJ*, 975, 83

Rieke, M. J., Kelly, D., & Horner, S. 2005, in SPIE, Vol. 5904, Cryogenic Optical Systems and Instruments XI, ed. J. B. Heaney & L. G. Burriesci, 1–8

Rieke, M. J., Kelly, D. M., Misselt, K., et al. 2023, *PASP*, 135, 028001

Rigby, J., Perrin, M., McElwain, M., et al. 2023, *PASP*, 135, 048001

Scholtz, J., Maiolino, R., D'Eugenio, F., et al. 2025, *A&A*, 697, A175

Secrest, N. J., Dudik, R. P., Dorland, B. N., et al. 2015, *ApJS*, 221, 12

Silk, J. 2013, *ApJ*, 772, 112

Souchay, J., Gattano, C., Andrei, A. H., et al. 2019, *A&A*, 624, A145

Swade, D., Bushouse, H., Greene, G., & Swam, M. 2014, in SPIE Conference Series, Vol. 9149, Observatory Operations: Strategies, Processes, and Systems V, ed. A. B. Peck, C. R. Benn, & R. L. Seaman, 914904

Taylor, M. B. 2005, in ASPCS, Vol. 347, Astronomical Data Analysis Software and Systems XIV, ed. P. Shopbell, M. Britton, & R. Ebert, 29

Übler, H., Maiolino, R., Pérez-González, P. G., et al. 2024, *MNRAS*, 531, 355

van der Wel, A., Franx, M., van Dokkum, P. G., et al. 2014, *ApJ*, 788, 28

Véron-Cetty, M. P. & Véron, P. 2003, *A&A*, 412, 399

Véron-Cetty, M. P. & Véron, P. 2006, *A&A*, 455, 773

Véron-Cetty, M. P. & Véron, P. 2010, *A&A*, 518, A10

Wagner, A. Y., Bicknell, G. V., & Umemura, M. 2012, *ApJ*, 757, 136

Whitney, A., Conselice, C. J., Bhatawdekar, R., & Duncan, K. 2019, *ApJ*, 887, 113

Wright, G. S., Rieke, G. H., Glasse, A., et al. 2023, *PASP*, 135, 048003

Wright, G. S., Wright, D., Goodson, G. B., et al. 2015, *PASP*, 127, 595

Wylezalek, D., Vayner, A., Rupke, D. S. N., et al. 2022, *ApJ*, 940, L7

Yang, G., Caputi, K. I., Papovich, C., et al. 2023, *ApJ*, 950, L5

Yue, M., Eilers, A.-C., Ananna, T. T., et al. 2024, *ApJ*, 974, L26

Zhang, L., Packham, C., Hicks, E. K. S., et al. 2024, *ApJ*, 974, 195

Appendix A: Object type mapping across catalogues

For consistency across catalogues, the object type flags were mapped to a unified scheme. Tables A.1–A.6 summarize all mappings used in the construction of the catalogue, where Original Code shows the classification as listed in the respective catalogues, Unified Type gives the corresponding mapping adopted in our catalogue, and Notes provide additional information from the original published catalogues regarding the abbreviations. Catalogues that did not provide objTypes (e.g. eFEDS, Swiftbat, and CDFS) are not listed here (see Sect. 3.6 for details).

Table A.1. Milliquas object type mapping.

Original code	Unified type	Notes
Q	QSO type1-BL	QSO, type-I broad-line core-dominated
A	AGN type1	AGN, type-I Seyferts/host-dominated
B	BL Lac	BL Lac type object
K	QSO-NL	NLQSO, type-II narrow-line core-dominated
N	AGN-NL	NLAGN, type-II Seyferts/host-dominated. Includes an unquantified residue of legacy NELGs/ELGs/LINERs, plus some unclear AGN.
S	Star	Star classified but showing quasar-like photometry and radio/X-ray association, thus included as a quasar candidate
R	R	Radio association flag
X	X	X-ray association flag
2	2	Double radio lobes displayed

Table A.2. Veroncat object type mapping.

Original code	Unified type	Notes
Q2	QSO type2	Type-2 QSO
S1	Seyfert 1	Seyfert 1 spectrum
S1h	Seyfert 1 –h	Broad polarized Balmer lines detected
S1i	Seyfert 1 –i	Broad Paschen lines observed in the infrared
S1n	Seyfert 1-NL	Narrow-line Seyfert 1
S1.0	Seyfert 1.0	
S1.2	Seyfert 1.2	
S1.5	Seyfert 1.5	
S1.8	Seyfert 1.8	
S1.9	Seyfert 1.9	
S2	Seyfert 2	Seyfert 2 spectrum
S2?	Seyfert 2 ?	Probable Seyfert 2
S3	Seyfert 3/LINER	Seyfert 3 or liner
S3b	Seyfert 3/LINER –b	Seyfert 3 or liner with broad Balmer lines
S3h	Seyfert 3/LINER –h	Seyfert 3 or liner with broad polarized Balmer lines detected
S	Seyfert (unclassified)	unclassified Seyfert
S?	Seyfert ?	Probable Seyfert
H2	Nuclear HII region	nuclear HII region
HP	High polarization	high optical polarization (>3%)
BL	BL Lac	Confirmed BL Lac
BL?	BL Lac ?	Probable BL Lac
?	BL Lac ??	Questionable BL Lac

Table A.3. MaNGA object type mapping.

Original code	Unified type	Notes
BROAD_agn	BROAD_agn	AGN identified by broad lines
BAT_agn	BAT_agn	AGN identified in <i>Swift</i> /BAT hard X-ray survey
WISE_agn	WISE_agn	AGN identified via WISE mid-IR colours
RADIO_agn (HERG)	HERG (quasar mode)	quasar-mode high-excitation radio galaxy
RADIO_agn (LERG)	LERG (radio mode)	radio-mode low-excitation radio galaxy

Table A.4. Rosat object type mapping.

Original code	Unified type	Notes
QSO	QSO	object with broad lines and $M_B < -22.5$
A	AGN-NL	narrow line objects with $[\text{OIII}]/\text{H}\beta > 2.0$ and/or $[\text{NII}]/\text{H}\alpha > 0.6$
BA	AGN-BL	objects with broad lines and $M_B > -22.5$
H	Starburst	starbursts with $[\text{OIII}]/\text{H}\beta < 2.0$ and/or $[\text{NII}]/\text{H}\alpha < 0.6$
G	Galaxy	galaxies (objects with no emission lines and Ca II break contrasts $> 30\%$)
B	BL Lac	BL Lacs
S	Star	
Cl	Cluster candidate	possible clusters (based on the proximity of a known cluster)
rad	Radio source	Catalogued radio source
Sy	Seyfert	
Irs	Infrared source	Identified via IR emission
Vis	Optical source	Optical/Visible classification
UvE	UV-excess source	UV-excess detection

Table A.5. BASS object type mapping.

Original code	Unified type	Notes
Sy1	Seyfert 1	AGN with broad $\text{H}\beta$
Sy1.9	Seyfert 1.9	AGN with narrow $\text{H}\beta$ and broad $\text{H}\alpha$
Sy2	Seyfert 2	AGN with narrow $\text{H}\beta$ and $\text{H}\alpha$
BZQ	Blazar – quasar type	beamed AGN with the presence of broad lines
BZG	Blazar – galaxy dominated	beamed AGN with only Host-galaxy features, no broad lines
BZB	Blazar – featureless cont.	beamed AGN, traditional continuum dominated blazars with no emission lines or host galaxy features

Table A.6. Stripe object type mapping.

Original code	Unified type
1	Stars
2	Ellipticals
3	Spirals
4	Type 2
5	Starbursts
6	Type 1
7	QSOs

Appendix B: Summary of catalogues

Table B.1. Summary of the catalogues used.

Catalogue Name	# AGNs	Redshift Range	Area (deg ²)	Info
Milliquas	1,021,800	0.001 - 7.642	–	AGNs from different surveys.
MaNGA	398	0.001 - 0.149	2,700 (MaNGA Field)	Multi-wavelength AGNs.
eFEDs	22,079	0.004 - 8.000	142	X-ray AGNs.
Stripe	2,459	0.000 - 7.011	31.3	X-ray AGNs with multi-wavelength counterparts.
<i>Chandra</i>	711	0.034 - 4.762	484.2	X-ray AGNs.
BASS	858	0.001 - 3.656	All-sky (<i>Swift</i> /BAT)	Hard-X-ray AGNs from VLT.
Veroncat	34,231	0.001 - 5.870	–	AGNs from different surveys.
Rosat	294	0.002 - 4.715	All-sky (Rosat)	X-ray/radio AGNs.
<i>Gaia</i> -CRF3	1,614,173	–	All-sky (<i>Gaia</i>)	AGNs in <i>Gaia</i> DR3 identified by 17 different catalogues.
Swiftbat	277	< 0.06	All-sky (<i>Swift</i> /BAT)	X-ray AGNs.

Appendix C: Columns

Table C.1. Description of the columns.

Column Nr & Name	Description
(1) Name	Object Names from literature (reference source given in Reference column). Priority was given to information from Milliquas due to completeness. Names for CDFS objects were derived from their position in the HHMMSS.SS+DDMMSS.S. format. Names provided by eJWST should be taken with caution, because these are usually introduced by the proposer and typically do not follow a standard convention.
(2-3) RA/Dec (J2000, deg)	Target coordinates (J2000, in degrees) from literature. Rounded to 7 decimals for display purposes and to avoid truncation. To see real accuracy, go to corresponding catalogue coordinate column (RA (catalogue)/Dec (catalogue)). Coordinates taken from <i>Gaia</i> were shifted to J2000. See Sect. 3.4 for more information.
(4) objType	Classification of the source (e.g. Seyfert, QSO, BL Lac, LINER, etc.), retrieved from proposer descriptions for targeted AGNs and from catalogues for non-targeted AGNs. Catalogue-specific codes were harmonized into a unified scheme; ‘NL’ and ‘BL’ indicate narrow-line or broad-line objects, ‘?’ marks uncertain types, and ‘??’ highly questionable classifications. Proposer Descriptions are kept as provided by the eJWST archive.
(5) Ref	Original publication used to determine first four columns. When an object was listed in multiple catalogues, the following priority was used (from left to right): Milliquas - MaNGA - eFEDs - Stripe - CDFS - BASS - Veroncat - Rosat - eJWST - <i>Gaia</i> - Swiftbat. This order was determined by how complete, updated and accurate the information from the individual catalogues were. All catalogues that do not provide reliable (or any) redshifts for the sources were placed close to the bottom.
(6) z	Redshift from literature. Retrieved either from NED or directly from the catalogues used. NED values were given priority. See Sect. 3.5 for more information. Missing redshifts were marked as NaN.
(7) zType	Technique by which the redshift was determined. Information were taken from NED (using its standard convention) or, if unavailable, from the catalogues. NED values were given priority. Catalogue-specific terms were harmonized to a common scheme (spectroscopic = ‘S’, photometric = ‘P’) to be consistent with the NED convention; unknown cases are marked with ‘U’.
(8) zRef	Redshift reference in the form of a bibcode for each object. Values were taken from NED when available, otherwise from the respective catalogues.

Table C.1. Continued.

Column Nr & Name	Description
(9) zNED	Flag indicating whether redshift information was taken from NED ('y') or not ('n').
(10) Observation ID	Unique identifier for an observation.
(11) Instrument	Name of the instrument used for this observation.
(12) Aperture	Unique targetable fiducial point and its associated region per Instrument
(13) Exptype	Exposure type - type of data in the exposure.
(14) Filter	Bandpass filters in different wavelengths.
(15) Calibrationlevel	Calibration level with Planned observations = -1 and Science-ready observations = 3
(16) Exptime (s)	Total exposure time.
(17) Public	States if the observation is public or not (True or False). Public = for all available, otherwise restricted to proposer for a certain period of time.
(18) Proposal ID	Collection-specific unique proposal identifier.
(19) Release Date (UTC)	Date the metadata for an observation is public (UTC).
(20) Intent	Intended purpose of observation (Science, Calibration, Background). Labelled as follows: Science = Scientific observations done with the purpose of targeting a specific object or area in the sky. Calibration = Observations used to calibrate the science instruments and observing modes. Background = Background observation listed by MAST portal or found through eJWST keywords.
(21) Central Wavelength (μ m)	Central wavelength of the observation.
(22) Targeted	Checks if object was targeted by JWST or not (True or False; see Sect. 3).
(23) Data Link	Link for direct data product download when observations are public.
(24) Proposal ID Link	Link to programme information for specific proposal ID.
(25) TSOVISIT	Flag indicating whether an observation is a TSO or not ('t' or 'f'). Nan values were assigned for observations not including this keyword on the eJWST archive.
(26) eJWST Name	Name of object as given by the proposer, listed as target_name in eJWST.
(27) RA (eJWST)	Right ascension in deg and J2000, listed as targetposition_coordinate_cval1 in eJWST.
(28) Dec (eJWST)	Declination in deg and J2000, listed as targetposition_coordinate_cval2 in eJWST. Note: These coordinates are found in jwst.observation, in jwst.archive the same keywords store the pointing coordinates of the instruments per observation.
(29) objType (eJWST)	Classification of object as listed by proposer in the eJWST archive.
(30) z (NED)	Redshift taken from the astronomical database NED by a coordinate search with 1 arcsec radius.
(31) zType (NED)	Technique used to determine the redshift. Information taken from the astronomical database NED by a coordinate search with 1 arcsec radius.
(32) zRef (NED)	Redshift Reference taken from the astronomical database NED by a coordinate search with 1 arcsec radius.
Name (*)	Name of object taken from (*) catalogue.
ID (*)	Source ID in (*) catalogue, when available.
RA (*)	Right Ascension in decimal degrees (J2000) taken from (*) catalogue.

Table C.1. Continued.

Column Nr & Name	Description
Dec (*)	Declination in decimal degrees (J2000) taken from (*) catalogue.
z (*)	Redshift taken from (*) catalogue, when available.
zType (*)	Technique used to determine the redshift. Information taken from (*) catalogue, when available. Spectroscopic redshift was labelled ‘spec’, photometric ‘phot’ and unknown cases ‘?’.
zRef (*)	Redshift Reference of object taken from (*) catalogue, when available.
objType (*)	Classification of object taken from (*) catalogue, when available.

(*) These fields are given for different catalogues. Depending on the AGN, they will correspond to one or several of the following:

- (33–41) Milliquas by [Flesch \(2023\)](#). Redshift type: spectroscopic with a precision better than 0.1; photometric when rounded to 0.1. Extra columns: XName (36) / RName (37) – Additional names from X-ray/Radio detections listed in Milliquas.
- (42–48) MaNGA by [Comerford et al. \(2024\)](#). Redshift type: spectroscopic.
- (49–55) eFEDS by [Liu et al. \(2022\)](#). Redshift type: from ‘CTP_REDSHIFT_GRADE’, with 5 = spectroscopic, 2–4 = photometric.
- (56–63) Stripe by [Ananna et al. \(2019\)](#). Name of object derived from their position in ‘JHHMMSS.SS+DDMMSS.SS’ format. Redshift type: spectroscopic. Extra columns: ID (Stripe) (57) - ID number for each source as assigned in [Lamassa et al. \(2016\)](#).
- (64–71) CDFS by [Luo et al. \(2017\)](#). Name of object derived from their position in ‘JHHMMSS.SS+DDMMSS.SS’ format. Redshift type: spectroscopic. Extra columns: ID (CDFS) (65) – X-ray Source ID.
- (72–79) BASS by [Koss et al. \(2022\)](#). Redshift type: spectroscopic when emission lines used (e.g. [O III], H α , Mg II, and CIV); ‘?’ otherwise. Extra columns: ID (BASS) (73) – catalogue ID in the BASS DR2 survey.
- (80–86) Veroncat by [Véron-Cetty & Véron \(2010\)](#). Redshift type: spectroscopic if ‘l_z’ column flagged by ‘*’; ‘?’ otherwise.
- (87–93) Rosat by [Brinkmann et al. \(2000\)](#). Redshift type: unknown, flagged as ‘?’.
- (94–96) *Gaia* by [Gaia Collaboration et al. \(2023\)](#). Coordinates transformed from J2016 coordinates. No redshifts.
- (97–99) Swiftbat by [Lutz et al. \(2018\)](#). No redshifts.

Table C.2. Sample lines of our JWST AGN catalogue.

Name	RA (J2000, deg)	Dec (J2000, deg)	objType	Ref	z	zType	zRef	zNED	Observation ID	Instrument	Aperture
NGC 4388	186.444683	12.661875	AGN-NL-R-X	Milquas	0.008419	SUN	1993ApJ...88...383L	y	jw09218003001_xx101_00001_miri	MIRI/IMAGE	MIRIM_SUB256
NGC 4388	186.444683	12.661875	AGN-NL-R-X	Milquas	0.008419	SUN	1993ApJ...88...383L	y	jw09218003001_xx102_00002_miri	MIRI/IMAGE	MIRIM_SUB256
NGC 4388	186.444683	12.661875	AGN-NL-R-X	Milquas	0.008419	SUN	1993ApJ...88...383L	y	jw09218003001_xx104_00004_miri	MIRI/IMAGE	MIRIM_SUB256
NGC 4388	186.444683	12.661875	AGN-NL-R-X	Milquas	0.008419	SUN	1993ApJ...88...383L	y	jw09218003001_xx105_00001_miri	MIRI/IMAGE	MIRIM_SUB256
NGC 4388	186.444683	12.661875	AGN-NL-R-X	Milquas	0.008419	SUN	1993ApJ...88...383L	y	jw09218003001_xx106_00002_miri	MIRI/IMAGE	MIRIM_SUB256
NGC 4388	186.444683	12.661875	AGN-NL-R-X	Milquas	0.008419	SUN	1993ApJ...88...383L	y	jw09218003001_xx108_00004_miri	MIRI/IMAGE	MIRIM_SUB256
NGC 4388	186.444683	12.661875	AGN-NL-R-X	Milquas	0.008419	SUN	1993ApJ...88...383L	y	jw09218003001_xx109_00001_miri	MIRI/IMAGE	MIRIM_SUB256
NGC 4388	186.444683	12.661875	AGN-NL-R-X	Milquas	0.008419	SUN	1993ApJ...88...383L	y	jw09218003001_xx10a_00002_miri	MIRI/IMAGE	MIRIM_SUB256
NGC 4388	186.444683	12.661875	AGN-NL-R-X	Milquas	0.008419	SUN	1993ApJ...88...383L	y	jw09218003001_xx10c_00004_miri	MIRI/IMAGE	MIRIM_SUB256
NGC 4395	186.453600	33.546860	AGN-NL-R-X	Milquas	0.001064	SUN	1998AJ...115...62H	y	jw02016-c-1007_1002_miri_ch1-shortmediumlong	MIRI/FU	MIRIFU_CHANNELIA
NGC 4395	186.453600	33.546860	AGN-NL-R-X	Milquas	0.001064	SUN	1998AJ...115...62H	y	jw02016-c-1007_1002_miri_ch2-shortmediumlong	MIRI/FU	MIRIFU_CHANNELIA
NGC 4395	186.453600	33.546860	AGN-NL-R-X	Milquas	0.001064	SUN	1998AJ...115...62H	y	jw02016-c-1007_1002_miri_ch3-shortmediumlong	MIRI/FU	MIRIFU_CHANNELIA
NGC 4395	186.453600	33.546860	AGN-NL-R-X	Milquas	0.001064	SUN	1998AJ...115...62H	y	jw02016-c-1007_1002_miri_ch4-shortmediumlong	MIRI/FU	MIRIFU_CHANNELIA
NGC 4395	186.453600	33.546860	AGN-NL-R-X	Milquas	0.001064	SUN	1998AJ...115...62H	y	jw02016-c-1002_1002_miri_ch1-shortmediumlong	MIRI/FU	MIRIFU_CHANNELIA
NGC 4395	186.453600	33.546860	AGN-NL-R-X	Milquas	0.001064	SUN	1998AJ...115...62H	y	jw02016-c-1002_1002_miri_ch2-shortmediumlong	MIRI/FU	MIRIFU_CHANNELIA
NGC 4395	186.453600	33.546860	AGN-NL-R-X	Milquas	0.001064	SUN	1998AJ...115...62H	y	jw02016-c-1002_1002_miri_ch3-shortmediumlong	MIRI/FU	MIRIFU_CHANNELIA
NGC 4395	186.453600	33.546860	AGN-NL-R-X	Milquas	0.001064	SUN	1998AJ...115...62H	y	jw02016-c-1002_1002_miri_ch4-shortmediumlong	MIRI/FU	MIRIFU_CHANNELIA
NGC 4395	186.453600	33.546860	AGN-NL-R-X	Milquas	0.001064	SUN	1998AJ...115...62H	y	jw02016-c-1003_1003_miri_ch1-shortmediumlong	MIRI/FU	MIRIFU_CHANNELIA
NGC 4395	186.453600	33.546860	AGN-NL-R-X	Milquas	0.001064	SUN	1998AJ...115...62H	y	jw02016-c-1003_1003_miri_ch2-shortmediumlong	MIRI/FU	MIRIFU_CHANNELIA
NGC 4395	186.453600	33.546860	AGN-NL-R-X	Milquas	0.001064	SUN	1998AJ...115...62H	y	jw02016-c-1003_1003_miri_ch3-shortmediumlong	MIRI/FU	MIRIFU_CHANNELIA
NGC 4395	186.453600	33.546860	AGN-NL-R-X	Milquas	0.001064	SUN	1998AJ...115...62H	y	jw02016-c-1003_1003_miri_ch4-shortmediumlong	MIRI/FU	MIRIFU_CHANNELIA
NGC 4395	186.453600	33.546860	AGN-NL-R-X	Milquas	0.001064	SUN	1998AJ...115...62H	y	jw02016-c-1002_1002_miri_nirspec_g235h-f170lp	NIRSPEC/IFU	NIRS_FULL_IFU
NGC 4395	186.453600	33.546860	AGN-NL-R-X	Milquas	0.001064	SUN	1998AJ...115...62H	y	jw02016-c-1002_1001_miri_nirspec_g395h-f290lp	MIRI/FU	MIRIFU_CHANNELIA
NGC 4395	186.453600	33.546860	AGN-NL-R-X	Milquas	0.001064	SUN	1998AJ...115...62H	y	jw02016-c-1002_1002_miri_ch1-shortmediumlong	MIRI/FU	MIRIFU_CHANNELIA
NGC 4395	186.453600	33.546860	AGN-NL-R-X	Milquas	0.001064	SUN	1998AJ...115...62H	y	jw02016-c-1002_1002_miri_ch2-shortmediumlong	MIRI/FU	MIRIFU_CHANNELIA
NGC 4395	186.453600	33.546860	AGN-NL-R-X	Milquas	0.001064	SUN	1998AJ...115...62H	y	jw02016-c-1002_1002_miri_ch3-shortmediumlong	MIRI/FU	MIRIFU_CHANNELIA
NGC 4395	186.453600	33.546860	AGN-NL-R-X	Milquas	0.001064	SUN	1998AJ...115...62H	y	jw02016-c-1002_1002_miri_ch4-shortmediumlong	MIRI/FU	MIRIFU_CHANNELIA
NGC 4395	186.453600	33.546860	AGN-NL-R-X	Milquas	0.001064	SUN	1998AJ...115...62H	y	jw02016-c-1003_1003_miri_ch1-shortmediumlong	MIRI/FU	MIRIFU_CHANNELIA
NGC 4395	186.453600	33.546860	AGN-NL-R-X	Milquas	0.001064	SUN	1998AJ...115...62H	y	jw02016-c-1003_1003_miri_ch2-shortmediumlong	MIRI/FU	MIRIFU_CHANNELIA
NGC 4395	186.453600	33.546860	AGN-NL-R-X	Milquas	0.001064	SUN	1998AJ...115...62H	y	jw02016-c-1003_1003_miri_ch3-shortmediumlong	MIRI/FU	MIRIFU_CHANNELIA
NGC 4395	186.453600	33.546860	AGN-NL-R-X	Milquas	0.001064	SUN	1998AJ...115...62H	y	jw02016-c-1003_1003_miri_ch4-shortmediumlong	MIRI/FU	MIRIFU_CHANNELIA
NGC 4418	186.727583	-0.877612	AGN-NL-R-X	Milquas	0.007085	SLS	2016SDSSD_C...0000:	y	jw01991-c-1003_1003_miri_ch1-shortmediumlong	MIRI/FU	MIRIFU_CHANNELIA
NGC 4418	186.727583	-0.877612	AGN-NL-R-X	Milquas	0.007085	SLS	2016SDSSD_C...0000:	y	jw01991-c-1003_1003_miri_ch2-shortmediumlong	MIRI/FU	MIRIFU_CHANNELIA
NGC 4418	186.727583	-0.877612	AGN-NL-R-X	Milquas	0.007085	SLS	2016SDSSD_C...0000:	y	jw01991-c-1003_1003_miri_ch3-shortmediumlong	MIRI/FU	MIRIFU_CHANNELIA
NGC 4418	186.727583	-0.877612	AGN-NL-R-X	Milquas	0.007085	SLS	2016SDSSD_C...0000:	y	jw01991-c-1003_1003_miri_ch4-shortmediumlong	MIRI/FU	MIRIFU_CHANNELIA
NGC 4418	186.727583	-0.877612	AGN-NL-R-X	Milquas	0.007085	SLS	2016SDSSD_C...0000:	y	jw01991-c-1003_1003_miri_f100w-sub256	MIRI/IMAGE	MIRI/IMAGE
NGC 4418	186.727583	-0.877612	AGN-NL-R-X	Milquas	0.007085	SLS	2016SDSSD_C...0000:	y	jw01991-c-0007_1004_miri_f1130w-sub256	MIRI/IMAGE	MIRI/IMAGE
NGC 4418	186.727583	-0.877612	AGN-NL-R-X	Milquas	0.007085	SLS	2016SDSSD_C...0000:	y	jw01991-c-0006_1003_miri_ch1-shortmediumlong	MIRI/FU	MIRIFU_CHANNELIA
NGC 4418	186.727583	-0.877612	AGN-NL-R-X	Milquas	0.007085	SLS	2016SDSSD_C...0000:	y	jw01991-c-0006_1003_miri_ch2-shortmediumlong	MIRI/FU	MIRIFU_CHANNELIA
NGC 4418	186.727583	-0.877612	AGN-NL-R-X	Milquas	0.007085	SLS	2016SDSSD_C...0000:	y	jw01991-c-0006_1003_miri_ch3-shortmediumlong	MIRI/FU	MIRIFU_CHANNELIA
NGC 4418	186.727583	-0.877612	AGN-NL-R-X	Milquas	0.007085	SLS	2016SDSSD_C...0000:	y	jw01991-c-0006_1003_miri_ch4-shortmediumlong	MIRI/FU	MIRIFU_CHANNELIA
NGC 4418	186.727583	-0.877612	AGN-NL-R-X	Milquas	0.007085	SLS	2016SDSSD_C...0000:	y	jw01991-c-0007_1004_miri_f1170w-sub256	MIRI/IMAGE	MIRI/IMAGE
NGC 4418	186.727583	-0.877612	AGN-NL-R-X	Milquas	0.007085	SLS	2016SDSSD_C...0000:	y	jw01991-c-0008_1006_miri_nirspec_g395m-f290lp	NIRSPEC/IFU	NIRS_FULL_IFU
NGC 4418	186.727583	-0.877612	AGN-NL-R-X	Veroncat	0.000237	SUN	1995ApJ...438...135K	y	jw07763006001_xx101_00001_nircam	NIRCAM/IMAGE	NIRCALL_FULL
NGC 4418	186.727583	-0.877612	AGN-NL-R-X	Veroncat	0.000237	SUN	1995ApJ...438...135K	y	jw07763006001_xx102_00002_nircam	NIRCAM/IMAGE	NIRCALL_FULL
NGC 4418	186.727583	-0.877612	AGN-NL-R-X	Veroncat	0.000237	SUN	1995ApJ...438...135K	y	jw07763006001_xx103_00003_nircam	NIRCAM/IMAGE	NIRCALL_FULL
NGC 4418	186.727583	-0.877612	AGN-NL-R-X	Veroncat	0.000237	SUN	1995ApJ...438...135K	y	jw07763006001_xx104_00004_nircam	NIRCAM/IMAGE	NIRCALL_FULL

Notes. Column (1): Name adopted from literature. Column (2-3): Right Ascension and Declination in decimal degrees, based on J2000 epoch. Column (4): Object Type adopted from literature and the eJWST archive. Column (5): Source of information for columns 1-4. Column (6): Redshift, taken either from NED or from the same source as in column 5. Column (7): Redshift type/method. Column (8): Redshift reference. Column (9): NED flag, indicating whether the redshift was taken from NED (y) or from the same source as listed in column 5 (n). Column (10): Unique identifier for an observation. Columns (11-12): Observation specific information. A detailed description of this table's contents is given in Table C.1.